methane (*26*). The isotopically heavy extractable organic matter in the Murray meteorite ($\delta^{13}C$, −5.3 per mil) may have resulted from some such high-temperature equilibration.

We believe that the $^{13}C/^{12}C$ data presented here are the first indication of a nonrandom isotopic distribution of carbon in meteorites. This property can now be included among others in descriptions of the generic relationships of the carbonaceous chondrites. The data strongly suggest that both oxidized and reduced forms of carbon are indigenous to the meteorites. The data also show which fractions are the least contaminated by terrestrial carbon.

J. W. SMITH*
I. R. KAPLAN
Institute of Geophysics and Planetary Physics, University of California, Los Angeles 90024

References and Notes

1. J. J. Berzelius, *Ann. Phys. Chem.* **33**, 113 (1834); F. Wohler, *Sitz. Akad. Wiss. Wien Math. Naturwiss. Kl.* **41**, 7 (1859).
2. G. Mueller, *Geochim. Cosmochim. Acta* **4**, 1 (1953).
3. It is not possible to reference all the published work here; two recent reviews are: H. C. Urey, *Science* **151**, 157 (1966); J. M. Hayes, *Geochim. Cosmochim. Acta* **31**, 1395 (1967).
4. W. G. Meinschein, B. Nagy, D. J. Hennessy, *Ann. N.Y. Acad. Sci.* **108**, 553 (1963).
5. M. C. Bitz and B. Nagy, *Proc. Nat. Acad. Sci. U.S.* **56**, 1383 (1966).
6. E. Anders, *Ann. N.Y. Acad. Sci.* **93**, 651 (1962); P. B. Hamilton, *Nature* **205**, 284 (1964); J. Oro and M. B. Skewes, *ibid.* **207**, 1042 (1965).
7. G. Boato, *Geochim. Cosmochim. Acta* **6**, 209 (1954).
8. H. Craig, *ibid.* **3**, 53 (1953).
9. R. N. Clayton, *Science* **140**, 192 (1963).
10. B. Nagy, *Proc. Nat. Acad. Sci. U.S.* **56**, 389 (1966); H. R. Krouse and V. E. Modzeleski, *Geochim. Cosmochim. Acta*, in press.
11. A. P. Vinogradov, O. I. Kropotova, G. P. Vdovykin, V. A. Grinenko, *Geokhimiya* **3**, 267 (1967).
12. The isotopic abundance may be defined as
$$\delta^{13}C\ \text{mil} = 1000 \times \frac{^{13}C/^{12}C\ \text{sample} - {}^{13}C/^{12}C\ \text{std. (PDB)}}{^{13}C/^{12}C\ \text{std. (PDB)}}$$
where PDB is the Pee Dee belemnite standard.
13. E. T. Degens, *Geochemistry of Sediments* (Prentice-Hall, Englewood Cliffs, N.J., 1965).
14. Haripura meteorite was also analyzed, and the results are very similar to those for the Mokoia meteorite in all respects. Since it is generally considered that the Haripura meteorite is a type II carbonaceous chondrite, we may have analyzed a mislabeled specimen and therefore do not report the results here.
15. J. W. Smith, J. W. Schopf, I. R. Kaplan, *Geochim. Cosmochim. Acta*, in press.
16. T. G. Tornabene, thesis, University of Houston (1967).
17. B. Nagy and M. C. Bitz, *Arch. Biochem. Biophys.* **101**, 240 (1963).
18. D. W. Nooner and J. Oro, *Geochim. Cosmochim. Acta* **31**, 1359 (1967).
19. Because of the loss of sample during adduction, pristane and phytane were not determined in the Ivuna sample. The sharp maximum at C_{21} in the alkane distribution from this meteorite may be due to a branched or cyclic saturated hydrocarbon also seen in the crude extract from the Erakot meteorite.
20. T. Belsky and I. R. Kaplan, *Geochim. Cosmochim. Acta* **34**, 257 (1970).
21. P. H. Abelson and T. C. Hoering, *Proc. Nat. Acad. Sci. U.S.* **47**, 623 (1961); E. T. Degens, M. Behrendt, B. Gotthardt, E. Reppmann, *Deep-Sea Res.* **15**, 11 (1968).
22. S. R. Silverman, in *Isotopic and Cosmic Chemistry*, H. Craig, S. L. Miller, G. J. Wasserburg, Eds. (North-Holland, Amsterdam, 1964); T. C. Hoering, in *Researches in Geochemistry*, P. H. Abelson, Ed. (Wiley, New York, 1967), vol. 2.
23. D. A. Flory and J. Oro, personal communication.
24. W. D. Rosenfeld and S. R. Silverman, *Science* **130**, 1658 (1959).
25. Y. Bottinga, *Geochim. Cosmochim. Acta* **33**, 49 (1969).
26. M. O. Dayhoff, E. R. Lippincott, R. V. Eck, *Science* **146**, 1461 (1964); R. V. Eck, E. R. Lippincott, M. O. Dayhoff, Y. T. Pratt, *ibid.* **153**, 628 (1966).
27. We thank E. Ruth for valuable assistance. This study was performed under NASA grants NGR 05-007-221 and NGL 05-007-215. Contribution No. 823, Institute of Geophysics and Planetary Physics, UCLA.
* Permanent address: Division of Mineral Chemistry, Commonwealth Scientific and Industrial Research Organization, P.O. Box 175, Chatswood, New South Wales, Australia.

30 January 1970

■

Nonphotographic Alpha Autoradiography and Neutron-Induced Autoradiography

Abstract. *With a new combination of two techniques, (i) alpha-particle or fission fragment registration in thin polymer foils by etching and (ii) automatic counting and magnification of the etched perforations by local evaporation of a thin metal layer with an electric spark, the sensitivity of conventional photographic methods for determining quantity and spatial distribution of alpha emitters, fissile materials, and of elements undergoing (n, α) reactions can be drastically improved, without need for darkroom processing and microscopic evaluation.*

The conventional method for determining the quantity and spatial distribution of fissile materials in biological samples is α autoradiography by photographic nuclear track emulsion. This method, which may require exposure times of as much as several years (*1, 2*), not only delays research but also introduces new problems due to changes in the emulsion, such as fading or fogging, or to the limited half-life of some nuclides. A new imaging technique, neutron-induced autoradiography (NIAR), permits the results to be obtained within a few hours of sample preparation. The basic procedure may be illustrated by the following experiment designed to determine the quantity and distribution of ^{239}Pu in the tubular bone of a beagle dog.

A thin bone sample mounted on a glass slide was covered with a polycarbonate plastic film (*3*) 6 or 10 μm thick and was exposed to thermal neutrons in the thermal column of the Bulk Shielding Reactor at Oak Ridge National Laboratory. The film was then clamped between two nonetchable plastic retainer rings to simplify further handling. Submersion of the mounted film at 60°C in 28 percent KOH for 1 hour etched pinholes with a diameter of several micrometers at the location of each fission fragment impact. After the etched film was rinsed and dried, it was placed on a circular brass electrode similar to one recently described (*4*) but larger in diameter. The film was covered with a piece of aluminized Mylar with the aluminized side facing the etched film and making contact with an outer, grounded electrode. A positive charge of 500 volts was applied; the sparks that occurred through the perforations in the etched film were coupled to a portable scaler through a quenching circuit. Each spark caused the evaporation of aluminum from the aluminized Mylar in an area that was several orders of magnitude larger than the original hole in the detector film (*5*). Therefore, no multiple sparking occurred through individual holes and a plainly visible "replica" of the holes remained in the aluminum layer.

The local density of evaporated Al spots is proportional to the local concentration of fissile material, and the integral number of sparks in a given sample can be related to the total content of a fissile material in a layer roughly corresponding in thickness to the range of fission fragments in the sample. If the sample is very thin and the detection efficiency for fission fragments is 100 percent, a 2π geometry results in 1 spark (count) per fission, since there are two fission fragments per fission. The sensitivity of the tested bone sample was estimated to be approximately 0.9 spark per fission.

The neutron fluence must be adjusted to the concentration of the fissile material because too small a density of spots results in poor resolution of the image and poor counting statistics, whereas a density exceeding 3000 spots

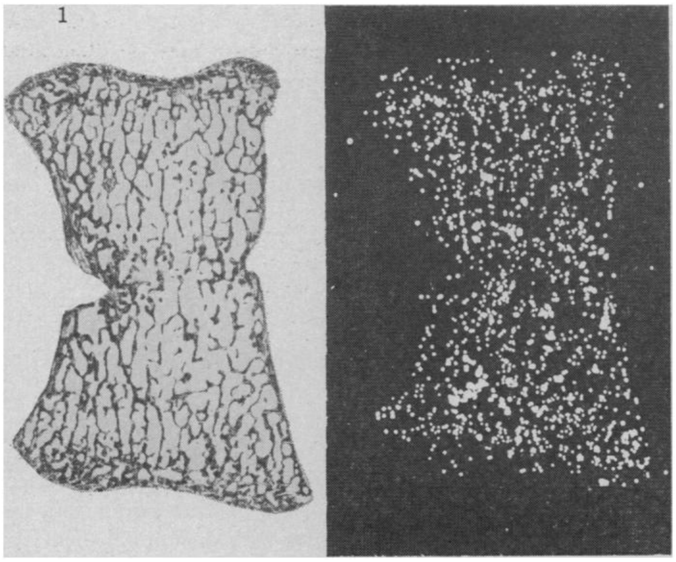

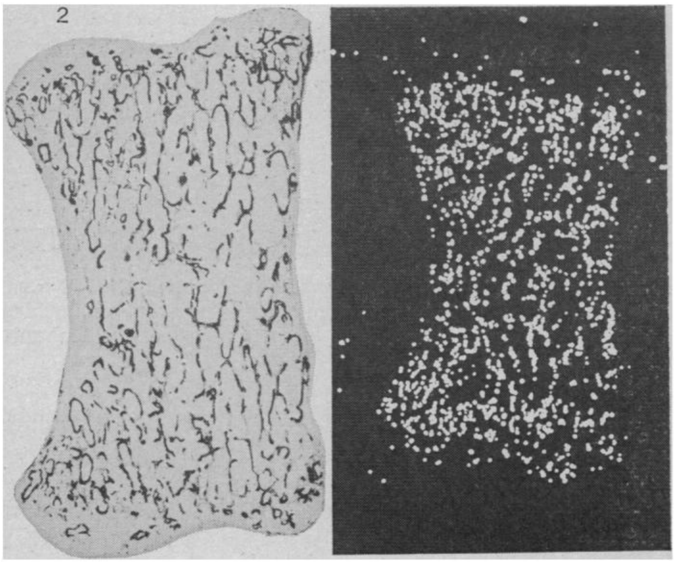

Fig. 1. (Left) Bone sample from a beagle containing approximately 9.5 pc/cm^2 of ^{239}Pu mounted on cellulose acetate foil. (Right) Sparked replica of an etched polycarbonate foil after exposure to thermal neutrons while in contact with the bone sample. Fig. 2. Alpha autoradiograph of beagle bone sample containing ^{226}Ra in a 15-μm cellulose nitrate foil: (left) after exposure time equivalent to that required for photographic α autoradiography and etching (without sparking); (right) spark image of the sample after reduction of exposure time by a factor of 30.

per square centimeter leads to an increasing number of overlapping spots and nonlinear response. Increasing the thickness of the Al layer or lowering the sparking voltage can decrease the spot diameter and extend the linear range somewhat, but this method is limited by the increasing probability of multiple sparking through the same etched hole if the area of evaporated Al becomes too small.

In the case of a typical ^{239}Pu-containing bone sample mounted on a glass slide and exposed to 5×10^{12} n/cm^2 (thermal), a total of 2000 sparks over the 1.27-cm^2 area of the bone sample, or 1580 sparks per square centimeter, were obtained. This number can be related to the activity a of ^{239}Pu per square centimeter of bone surface by the following equation:

$$a = \frac{K \times C \times A \times S}{N_0 \times \sigma \times \Phi}$$

where a is picocuries per square centimeter of ^{239}Pu; K is the correction factor for self-absorption and fission fragment detection efficiency (~ 0.9); C is counts per square centimeter (1580); A is atomic weight (239); S is the specific activity of ^{239}Pu (0.0617×10^{12} pc/g); σ is the cross section (740×10^{-24} cm^2); Φ is the neutron fluence, n/cm^2 (5×10^{12}); and N_0 is the Avogadro number (6.025×10^{23}). For the tested bone sample the resulting activity was approximately 9.5 pc/cm^2.

In other samples containing less ^{239}Pu and requiring a higher neutron fluence, the background caused by the natural uranium content of the glass slide became a limiting factor. In addition, a fairly intense, short-lived γ radioactivity was induced in the glass. Replacement of the glass by suitable plastics essentially eliminated the activation problem and reduced the background by about 2 orders of magnitude. Figure 1 shows an original bone sample mounted on a cellulose acetate foil and its neutron-induced autoradiograph.

If a film is "overexposed" with neutrons and slightly overetched, a very detailed image of the sample becomes directly visible in the etched film without sparking it. Similar "prints" have been obtained previously with thick Lexan foils that were exposed to neutrons in contact with certain minerals (*6*).

If fast neutrons are used, other fissile elements such as Th can also be detected. By preparing autoradiographs at different neutron energies, it is, in principle, possible to distinguish between extremely low concentrations of nuclides with different cross sections.

The registration efficiency for α particles is quite small in Kimfol and Lexan. More sensitive detector films are needed if imaging by sparking is employed in α autoradiography (for example, to determine Ra in bone or tissue or to use NIAR for (n, α) reactions to determine the quantity and distribution of elements such as Li and B in biological samples, minerals, alloys, and so forth). In carefully prepared and etched cellulose nitrate films, the registration efficiency for α particles from a thin ^{235}U α source can exceed 50 percent (*4*).

In α autoradiography studies of a beagle bone sample containing ^{226}Ra, for example, a high resolution, good contrast, directly visible autoradiograph is obtained without sparking, if the sample is exposed to a 15-μm cellulose nitrate film as long as required to obtain a photographic autoradiograph and etched for 2 hours in 28 percent KOH at 40°C (Fig. 2). The high α track density permits a significant reduction of exposure time if the sample is to be sparked for evaluation. A reduction by a factor of 30, for instance, still results in a good spark image (Fig. 2), and the spark count (2200) is sufficient for an accurate determination of its ^{226}Ra content. Obviously, this technique permits a considerable reduction in exposure time (or increase in sensitivity), if high resolution is not required in quantitative experiments, and has the additional advantage of obviating the necessity for darkroom and microscope work. For samples containing fissile materials, it would replace exposure times of several months by an equal number of days, with no need for neutron exposure.

The principle of NIAR can also be used in a detector system for thermal and fast neutron radiography (imaging of neutron fluence distributions). A

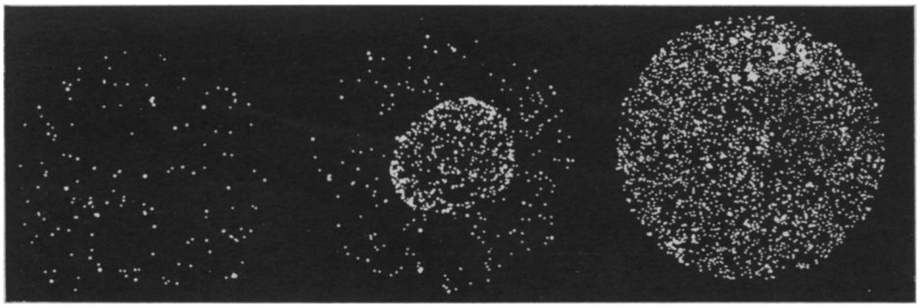

Fig. 3. Sparked replicas: (left) distilled water (1 cm^3) and (center) tap water (1 cm^3), evaporated on polycarbonate films before irradiation, etching, and spark counting; (right) a filter through which 8 m^3 of air passed (field diameter, 20 mm).

combination of a detector film with either a thin fissile converter foil or a material undergoing (n, α) reactions has been used in such experiments. The choice of additional, selective absorber foils such as Cd permits the use of certain neutron energies. The high sensitivity of NIAR permits the use of low neutron fluences. If a ^{235}U converter foil is employed, as few as 10^7 fast or 10^5 thermal neutrons per square centimeter cause approximately 100 detector holes per square centimeter, resulting in sufficient contrast and resolution for many cases. Other advantages are that this detector system, unlike the widely used photographic film, is almost insensitive to γ and β radiation, it needs no darkroom processing, and many replicas can be made quickly from the original etched film by repeated sparking of new aluminized Mylar foils. The replicas can be used directly as slides or as "negatives" for photographic enlargements. A spark counter with a larger diameter has been used for neutron radiography experiments.

There are several other applications of this technique. One is the ultrasensitive determination of fissile materials in liquids and gases. Such an application is illustrated in Fig. 3: 1 cm^3 of distilled water and 1 cm^3 of Oak Ridge tap water were evaporated on a detector film before exposure to a thermal neutron fluence of 1.33×10^{15} n/cm^2. The distilled water showed essentially background (150 sparks), whereas the tap water sample exhibited 650 sparks in a well-defined spot, corresponding to 1.4×10^{-13} g of natural uranium per cubic centimeter of water. This method is considerably more sensitive, more accurate, and more convenient than is the microscopic counting method because tracks in a much larger area can be completely counted in a short time. With microscopic counting, a detection limit of about 2×10^{-12} g/cm^3 has been claimed for uranium (*7*), whereas in our experiments the sensitivity was at least a factor of 100 better, with a further increase easily possible.

If untreated urine is evaporated on a detector film, a relatively thick layer of solid residue (mostly organic) remains and causes self-absorption of the fission fragments. This difficulty might be overcome by destruction of the organic material before evaporation of the sample or by the use of smaller or diluted urine samples on the film.

Figure 3 also shows the spark replica of a standard piece of Whatman filter paper through which 8 m^3 of air had passed. Obviously, the method is sensitive enough for accurate measurements of the natural concentration of fissile materials in air. With α-sensitive foils, B, Li, and other elements, in liquids and gases could be measured in a similar manner. The high sensitivity of the method may permit its use for tracer studies in hydrology, meteorology, and ecology.

KLAUS BECKER, D. R. JOHNSON
Health Physics Division,
Oak Ridge National Laboratory,
Oak Ridge, Tennessee 37830

References and Notes

1. W. S. S. Jee, in *Assessment of Radioactivity in Man* (International Atomic Energy Agency, Vienna, 1965), p. 369.
2. R. E. Rowland and J. E. Farnham, in *ANL-7489* (Argonne National Laboratory, Argonne, Ill., 1968), p. 33.
3. Film name: Makrofol, Bayer AG, Leverkusen, Germany; produced in the United States under the name Kimfol by Kimberly-Clark, Lee, Mass.
4. D. R. Johnson, R. H. Boyett, K. Becker, *Health Phys.*, in press.
5. W. J. Cross and L. Tommasino, in *Proceedings of the International Conference on Nuclear Track Registration in Solids* (Univ. of Clermont-Ferrand, France, 1969), sect. III, p. 73.
6. J. D. Kleeman and J. F. Lovering, *Science* **156**, 512 (1967); ———, in *Proceedings of the International Conference on Nuclear Track Registration in Solids* (Univ. of Clermont-Ferrand, France, 1969), sect. VI, p. 41.
7. R. L. Fleischer and D. B. Lovett, *Gen. Elec. Tech. Inform. Ser. 68-C-098* (1968).
8. The bone samples were obtained from W. S. S. Jee, University of Utah, Salt Lake City. Research sponsored by the U.S. Atomic Energy Commission under contract with the Union Carbide Corporation.

20 October 1969

Saturn's Rings: Identification of Water Frost

Abstract. *A recently published infrared spectrum of Saturn's rings resembles our laboratory spectra of water frosts. Furthermore, there are discrepancies between the ring spectrum and ammonia frost spectra in the 2- to 2.5-μ region. These discrepancies render unlikely a reported identification of ammonia frost in the ring spectrum.*

Kuiper, Cruikshank, and Fink (*1*) reported a conclusive identification of ammonia ice in the rings of Saturn. They obtained a new reflection spectrum of the rings with a Fourier-transform spectrometer. Comparing the ring spectrum with an unpublished laboratory spectrum of NH_3 frost in the 1.2- to 2.6-μ region, they identified eight ring spectral features as due to frozen ammonia. Earlier Cruikshank (*2*) had made a tentative identification of frozen ammonia based largely on a "1.66-μ band" in a ring spectrum of Mertz and Coleman (*3*). The new ring spectrum of Kuiper *et al.* shows several additional prominent bands (particularly near 1.5 μ and between 2.0 and 2.5 μ) reported to correspond to ammonia features. Also assigned to ammonia ice are a possible weak feature near 1.26 μ and a broad feature beyond 3 μ.

However, our laboratory data show that H_2O frost spectra also resemble the spectrum of Saturn's rings, and in fact present better agreement with the ring spectrum than does NH_3 frost. But conclusive identification of H_2O frost in the rings is premature.

For purposes of comparison with laboratory data, we present in Fig. 1 (curve III) a ratio of the Saturn ring spectrum to the lunar comparison spectrum also reported by Kuiper *et al.* Curve III is a ring spectrum corrected for atmospheric transmission and instrument response, assuming that the telluric absorption bands are of equal strength in the two spectra and that the spectra were measured with the same instrumentation. If we assume that the moon has no reflectance features in this region that are comparable in strength to the observed features in the ring spectrum, then the features in curve III are due to the ring.

In the upper portion of Fig. 1 we compare the new spectrum of Saturn's rings (curves I and III) with a reflection spectrum for a fine-grained H_2O frost (curve II) observed in the laboratory by one of us [H.H.K. (*4*)].